Automation of Impedance Measurement for Harmonic Stability Assessment of MMC-HVDC Systems

Yang, Dongsheng; Wang, Xiongfei; Ndreco, Mario; Winter, Wilhelm; Juhlin, Robert; Krontiris, Athanasios

Published in:
18th International Workshop on Large-scale Integration of Wind Power into Power Systems as well as on Transmission Networks for Offshore Wind Power Plants

Publication date:
2019

Document Version
Accepted author manuscript, peer reviewed version

Automation of Impedance Measurement for Harmonic Stability Assessment of MMC-HVDC Systems

Dongsheng Yang, Xiongfei Wang
Department of Energy Technology,
Aalborg University
Pontoppidanstraede 111, Aalborg,
9220, Denmark
doy@et.aau.dk, xwa@et.aau.dk

Mario Ndreko, Wilhelm Winter
TenneT TSO GmbH,
Bernecker Straße 70, 95448,
Bayreuth, Germany
Mario.Ndreko@tennet.eu,
wilhelm.winter@tennet.eu

Robert Juhlin, Athanasios Krontiris
ABB AG,
Kallstadter Straße 1,
Mannheim, Germany
robert.juhlin@se.abb.com
athanasios.krontiris@de.abb.com

***Abstract*—Modular Multilevel Converter-High-Voltage Direct Current (MMC-HVDC) transmission systems can interact with the grid impedance, leading to harmonic instability phenomena. To screen the risk of harmonic instability in multi-vendor MMC-HVDC-based transmission systems, an automated impedance measurement toolbox is developed for Transmission System Operator (TSO), which allows the TSO to extract the harmonic impedance model directly from the vendor-specified black-box electromagnetic transient models of MMC-HVDC systems. The automated toolbox can be seamlessly incorporated with the PSCAD software environment, and it is benchmarked in two steps in this work: first for a generic MMC system against its analytically derived impedance, and then for a vendor-specific MMC installation against the model used by the vendor. Finally, the application of the toolbox for a generic HVDC system tested in a transmission power network is presented.**

Keywords—MMC-HVDC, Harmonic instability, Impedance Measurement, Automation.

I. INTRODUCTION

Modular multilevel converters (MMCs) have been widely used in the high-voltage direct current (HVDC) transmission systems, thanks to its modularity, scalability, and flexibility [1]. MMC-HVDC transmission systems built by different vendors are being installed and interoperated in modern power transmission grid. However, the interactions between the wideband control loops of MMCs and the grid impedance poses may give rise to abnormal harmonics or even oscillations in different frequency ranges, which is also known as harmonic instability [2]. In 2016, Transmission system operator (TSO) TenneT reported a 451 Hz resonance phenomenon in one of the North Sea offshore wind farms that use MMC-HVDC transmission [3]. In 2017, China Southern Power Grid reported a 1270 Hz resonance between MMC-HVDC Converter and AC Grid in Luxi, China [4]. These resonances bring in various challenges, including capacitor and cable damage due to overvoltage, and the disconnection of transmission lines, which cause significant economic losses and severely threaten the security and quality of the electricity supply.

In order to secure the reliable operation of modern power transmission systems, the identification and quantification of interaction modes between the MMC-HVDC stations and the grid resonance at the point of connection (PoC) become essential.

The Electromagnetic Transient (EMT) simulation is nowadays a common practice for evaluating the harmonic stability of HVDC systems. However, the obtained EMT simulation results are case-dependent and cannot provide little insight into stability margins. To address the challenges with the EMT simulations, there are two general practices for the harmonic stability assessment of MMC-HVDC systems. First, the modal analysis based on the state-space model in the time domain [5], and second, the impedance-based analysis based on impedance models used in the frequency domain [6]. The modal analysis based on the state-space model provide full observability of oscillation modes and their damping ratios. It is also easier to implement for large and complex networks. However, it usually requires a prior knowledge on the system parameters, which are difficult to obtain for TSOs.

The impedance-based analysis enables, by default, to characterize the dynamic behavior of MMC-HVDC stations at the PoC. The impedance model of MMC can be obtained either based on the analytical modeling, or by applying the frequency scan at the PoC of MMC. Then, the interactions between the MMC-HVDC and power grids can be analyzed by comparing the impedance model of the MMC and the grid impedance. A remarkable advantage of the impedance-based analysis lies in that no prior knowledge on the control system and hardware structure of the MMC-HVDC are needed, which allows TSOs to screen the risk of oscillations by measuring the impedance directly from the (vendor-specific) black-box EMT models of MMC-HVDC systems.

The contribution of this paper is an automated impedance measurement toolbox, using the frequency scan for obtaining the harmonic impedance model directly from (vendor-specific) black-box EMT models. In the toolbox, the whole process of impedance measurement is automated, considering the effects of switching noises, sideband harmonics, and other nonlinear parasitic that are inherent for the power electronic converters [7]. This allows TSOs to perform the harmonic stability analysis directly with the frequency domain measurement data, even without the background knowledge of power electronics and signal processing. Moreover, the impedance curves obtained by the toolbox can also be, in principle, used as the input for identifying state-space converter models, which can be further used in modal analysis of large-scale networks. In addition, this black-box impedance model provides a powerful language for TSOs and vendors to specify the dynamic behavior at the converter terminal, which is critical for the interoperability of multi-vendor MMC-HVDC systems.

II. Impedance-Based Harmonic Stability Analysis

Fig. 1 illustrates a generic system diagram of an MMC-HVDC station. A multiple-timescale control system is generally equipped with the MMC to regulate the current and power exchanged with the grid, which consists of circulating current suppression control (CCSC), voltage balance control (VBC) of the submodules, and ac current control (ACC), phase-locked loop (PLL). Moreover, the active power injected into the grid can be regulated either by the dc-link voltage control (DVC) or the active power control (APC), while the reactive power can be regulated either by the ac voltage magnitude control (AVC) or reactive power control (RPC). These control loops interact with the resonance frequencies of the ac grid impedance, which may lead to instabilities, resonances, or abnormal harmonics over a wide frequency range, depending on the net damping of the systems.

Fig.2 shows the equivalent circuit of the MMC-HVDC station, where the whole MMC converter is equivalently represented by a current source $\mathbf{i_c}$ and a parallel impedance $\mathbf{Z_c}$. In the frequency range that is far beyond the fundamental frequency of the grid, the impedance $\mathbf{Z_c}$ can be treated as single-input and single-output (SISO) transfer function. In this case, the harmonic stability caused by the interactions between MMC converter and ac grid impedance can be easily determined by checking where the minor loop gain $\mathbf{T_{minor}} = \mathbf{Z_g(s)/Z_c(s)}$ shown in Fig. 3 meets the Nyquist stability criterion.

In the near and below fundamental frequency range, however, the impedance $\mathbf{Z_c}$ is a multiple-input-multiple-output (MIMO) impedance matrix due to the frequency-coupling induced by the asymmetrical dynamics of the outer loops as well as the internal dynamics of the MMC submodules. Therefore, the generalized Nyquist stability criterion (GNC) has to be utilized to assess the system harmonic stability.

III. Impedance Measurement by Frequency Scanning

The principle of the impedance measurement by frequency scanning is shown in Fig. 4. The converter under test is treated as a black-box and the perturbation signals are injected into the system to extract the converter dynamics.

The magnitude of the perturbation signal has to be small enough to meet small-signal assumptions, but large enough to deal with noise and switching harmonics from the converter.

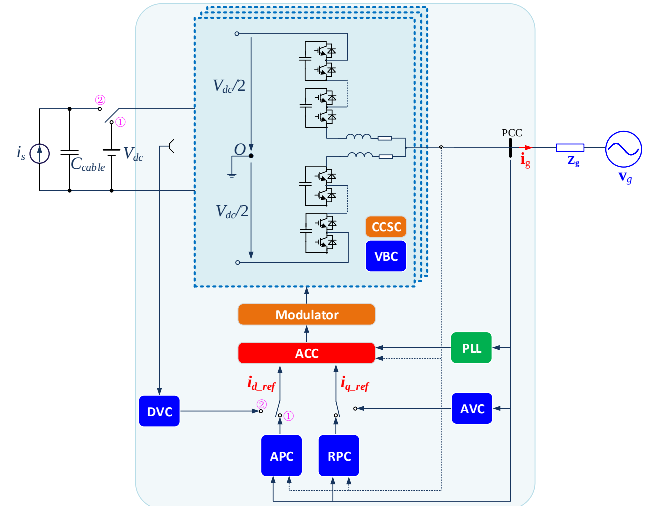

Fig. 1. System diagram of an MMC-HVDC station and ac grid.

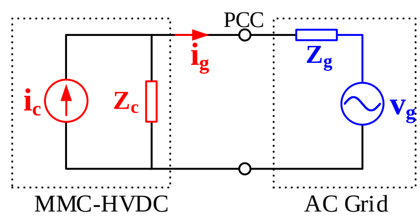

Fig. 2. Equivalent circuit of an MMC-HVDC station and ac grid.

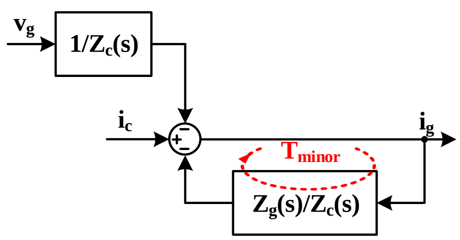

Fig. 3. Equivalent block diagram of an MMC-HVDC station and ac grid.

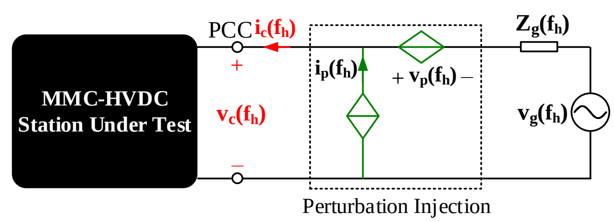

Fig. 4. Impedance measurement of MMC-HVDC using frequency scanning.

In general, the excitation magnitude is chosen between 1%~5% of steady-state values. Basically, there are two types of perturbation injection methods: shunt current injection and series voltage injection. To maximize the perturbation that flows into the converter-side, proper perturbation injection methods have to be selected according to the grid impedance. When the grid impedance is much larger than the converter impedance, most of the shunt current perturbation would flow into the converter side thus this injection method is preferable in this case. Otherwise, the series voltage injection method should be used.

Then, the currents $\mathbf{i_c}$ and voltages $\mathbf{v_c}$ at the converter terminal are measured and processed by Fast Fourier Transformation (FFT). Thus, the magnitude and phase angle of MMC converter impedance at the perturbation frequency can be calculated. In this project, the converter impedance is measured in stationary reference frame and single sinusoidal perturbation signal is used during the frequency scanning. Therefore, the SISO-impedance model can be calculated as:

$$\mathbf{Z_c}\left(f_h\right)=\frac{\mathbf{v_c}\left(f_h\right)}{\mathbf{i_c}\left(f_h\right)} \tag{1}$$

where $\mathbf{v_c}(f_h)$ and $\mathbf{i_c}(f_h)$ are the positive sequence components of three-phase converter voltages and current at the perturbation frequency f_h, i.e.,

$$\mathbf{v_c}\left(f_h\right)=\frac{1}{3}\begin{bmatrix}1 & e^{j\frac{2}{3}\pi} & e^{-j\frac{2}{3}\pi}\end{bmatrix}\begin{bmatrix}v_a\left(f_h\right)\\ v_b\left(f_h\right)\\ v_c\left(f_h\right)\end{bmatrix} \tag{2}$$

$$\mathbf{i_c}\left(f_h\right)=\frac{1}{3}\begin{bmatrix}1 & e^{j\frac{2}{3}\pi} & e^{-j\frac{2}{3}\pi}\end{bmatrix}\begin{bmatrix}i_a\left(f_h\right)\\ i_b\left(f_h\right)\\ i_c\left(f_h\right)\end{bmatrix} \tag{3}$$

As for the MIMO impedance matrix in the low-frequency range, the responses for one-frequency perturbation could contain both the perturbation-frequency component and various sideband-frequency components. To measure the cross-coupling impedance terms, the sideband-frequency component must be transformed into another frame so that it has the same frequency as the perturbation. Then the cross-coupling impedance terms can be measured in the same principle is the same as SISO impedance.

IV. General Framework of Impedance Measurement Automation

The automation toolbox is developed in the PSCAD software environment, as shown in Fig. 5, which contains the main script, PSCAD/self-defined automation library, PSCAD simulation file, and database.

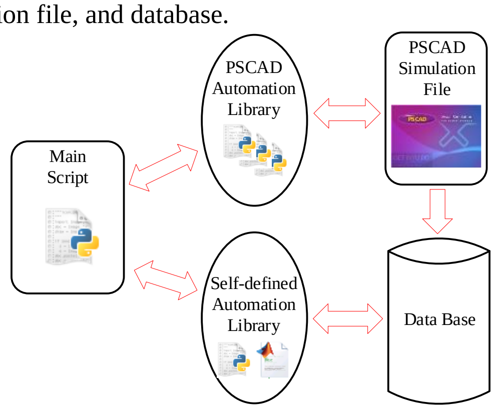

Fig. 5. Elements of impedance measurement toolbox

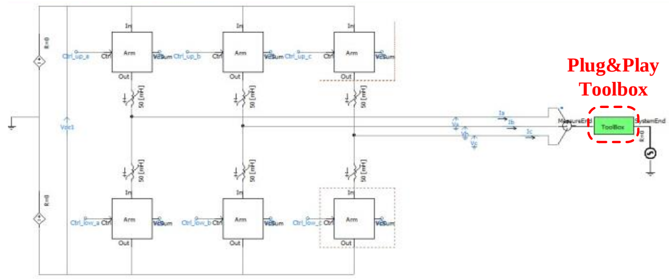

Fig. 6. Plug & play PSCAD toolbox for perturbation injection and data logging.

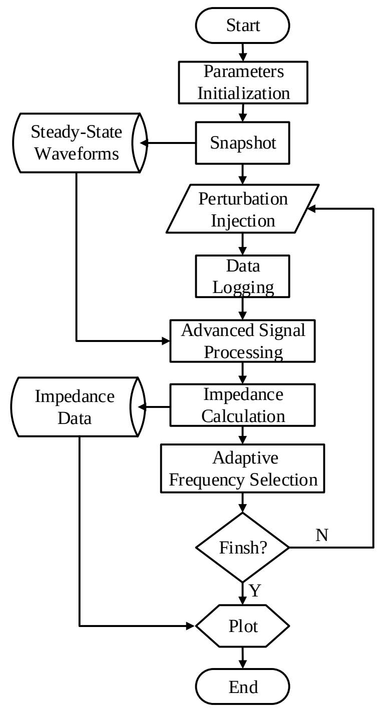

Fig. 7. Flowchart of the main script.

The main script is programmed in Python while the self-defined automation library is programmed using both Python and Matlab. The PSCAD automation library is provided by Manitoba Hydro International Ltd to interface with PSCAD simulation file. The database is used to save the steady-state and perturbed waveforms as well as their Fourier analysis results. The arrows indicate the communications among different elements. In the PSCAD simulation file, a plug and play PSCAD toolbox is developed for the perturbation injection and data-logging, which can be directly inserted at the terminal of the MMC converter, as shown in Fig. 6.

Among all the elements of the automation toolbox, the main script takes charge of all the procedures of the impedance measurement. By setting some initial parameters for the frequency scanning and simulation settings, the main script will execute all the procedures automatically without any human interference.

The flowchart of the main script is shown in Fig. 7. First, the main script starts with parameter initialization, then it opens the PSCAD simulation file through PSCAD automation library and runs the simulation until the system reaches the steady-state. Then a snapshot is captured to serve as the starting point for the subsequent frequency scanning. At the same time, the steady-state-waveforms are saved to the database for later switching harmonic elimination.

After that the main script enters into the loop program for frequency-scanning, which includes:

1) Perturbation injection. Inject the perturbations at the given perturbation frequency with the preset magnitude and injection method.

2) Data logging. The perturbed voltages and currents at the terminals are recorded and saved to the database.

3) Advanced signal processing. Both the perturbed waveforms and steady-state waveforms are processed to extract the converter dynamics from time-varying fundamental components, switching noise and the sideband harmonics. The major challenge lies in how to filter out the useful signals under extremely low signal-noise ratio (SNR). The advanced signal-processing functions are developed based on the power electronics knowledge in the self-defined automation library.

4) Impedance calculation. The frequency responses are calculated according to the principles illustrated in Section III, and recorded in the database.

5) Adaptive frequency selection. Since the large-scale system, EMT simulation in PSCAD is very time consuming, and adaptive frequency interval selection algorithm is implemented [8]. The frequency resolution is automatically selected to reduce the simulation time while maintaining accuracy.

After the scanning is finished, the frequency response of the output impedance will be plotted for harmonic stability analysis according to Section II. As shown in Fig. 8, the measured results are indicated by the circles and asterisks, which match well with the analytical impedance model based on the generic MMC-HVDC system.

V. Application of the Toolbox

A. Validation with the toolbox of a vendor

In order to validate the toolbox, it is used in combination with a vendor-specific black-box model of a real MMC-HVDC installation. The vendor uses a sweeping method to measure the impedance: the perturbation frequency that is injected changes continuously and covers the complete frequency range of interest. Certain filters are utilized to filter out the voltages and currents for other frequencies. The main benefit of the sweeping method is that it provides a continuous impedance with reasonable computation effort. Results from the toolbox described earlier in the paper are in good agreement with the vendor's sweeping method for the points selected by the algorithm described in Section IV, as shown in the Figs. 9 and 10.

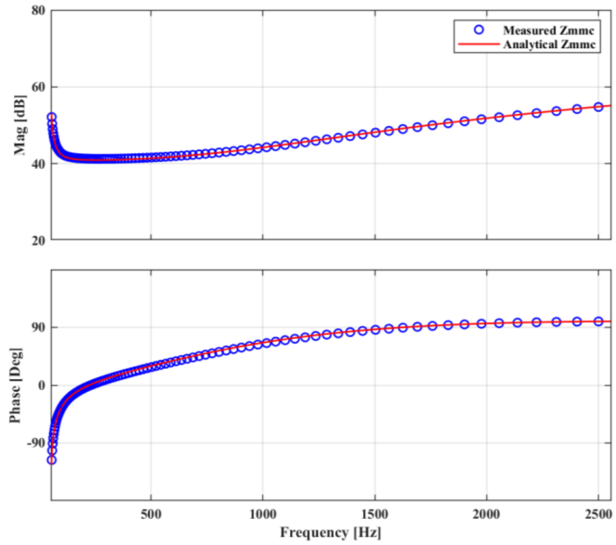

Fig. 8. Comparison of the measured impedance model with the analytical model based on the generic MMC-HVDC system.

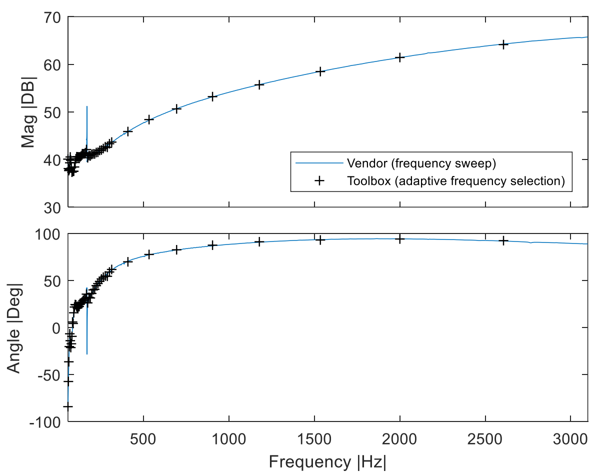

Fig. 9. Comparison of TSO's method with the vendor's sweeping method, wide frequency range

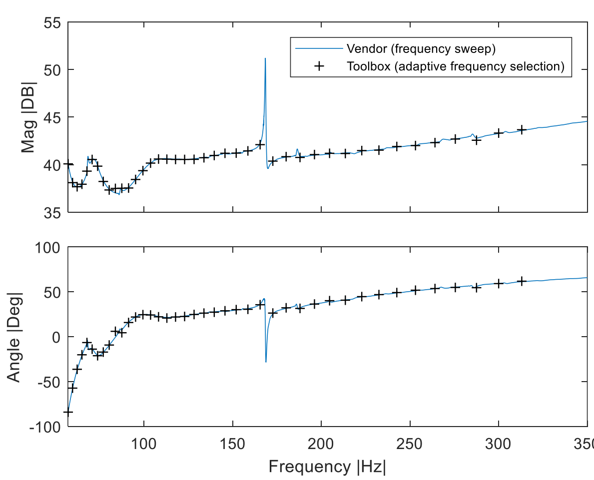

Fig. 10. Comparison of TSO's method with the vendor's sweeping method, narrow frequency range

Individually selected frequencies as in the TSO's method directly give accurate results for the selected frequencies. On the other hand, the method could miss rapid changes of impedance, as shown in Figure 10 around 168 Hz. The accuracy of the sweeping method depends on the speed at which the sweep is performed. A slower sweep takes longer simulation time, but it generally yields more accurate curves. However, even a moderately fast sweep can detect a rapid change in impedance, and the measurement could then be repeated over that interval with a slower sweeping speed.

B. Example on a generic use case

Fig. 11 shows the generic EMT model of MMC-HVDC station, where two different grid configurations are used for harmonic stability analysis. Fig. 11 shows the impedances of the grid and MMC station of the stable case, where the phase difference of the Z_g and Z_{mmc} are less than 180° at the intersection frequencies. Fig. 12 shows the impedances of the grid and MMC station of the unstable case, where the phase difference of Z_g and Z_{mmc} are larger than 180° at the intersection frequency 1890 Hz.

To verify the harmonic stability analysis in the frequency domain, nonlinear time domain EMT simulation are carried out, as shown in Fig. 14. Time domain simulation for energization of the MMC station are shown in Fig. 14 (a) and (b), where the PCC voltage and MMC output current are stable. The grid configuration at 5 s is changed which lead to an unstable case, as shown in Fig. 14 (c) and (d). The resonance is at 1887 Hz, as shown in Fig. 15, which matches well with the stability analysis in the frequency domain.

VI. CONCLUSION

An advanced toolbox is developed to automatize the harmonic impedance measurement of multi-vendor MMC-HVDC systems. It allows transmission system operators to extract the harmonic impedance directly from the vendor-specified black-box EMT models of MMC-HVDC converters, without prior knowledge on their hardware and control details. The general framework of harmonic impedance measurement is illustrated in this paper, and the applications of the toolbox using generic as well as vendor-specific HVDC systems is also presented.

Using the measured impedance, either directly in impedance-based stability analysis or, after some processing, in modal analysis, the risk of harmonic instability in MMC converters connected to real networks under various grid configurations can be accurately identified.

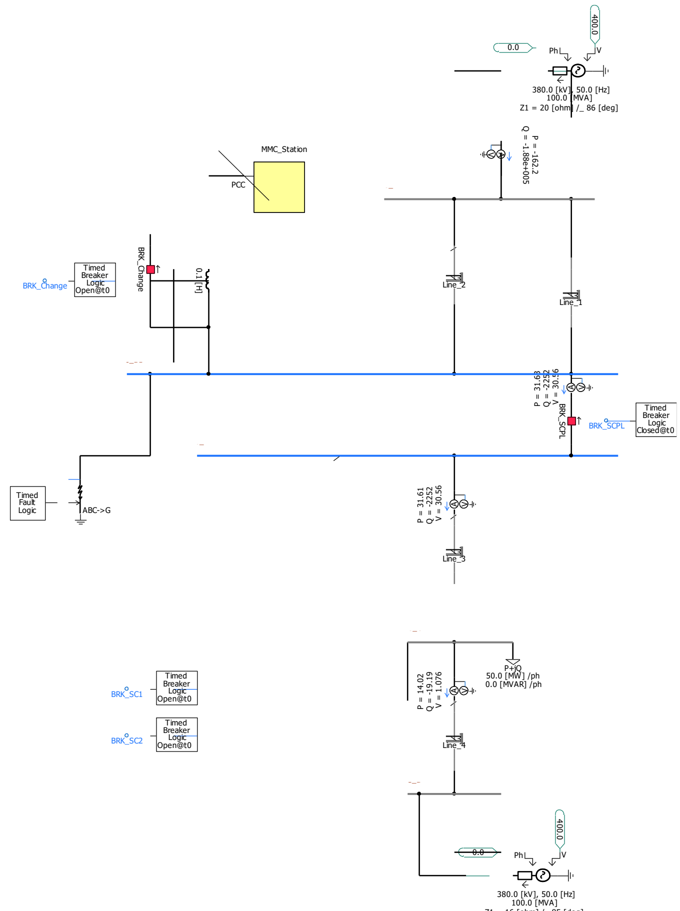

Fig. 11. Generic average EMT model of an MMC HVDC station.

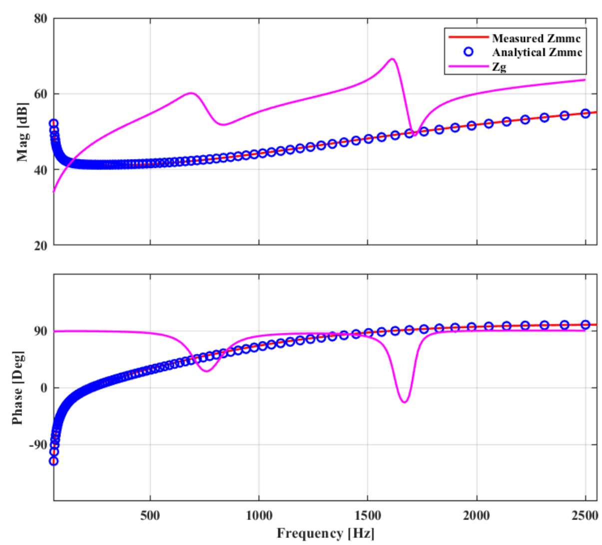

Fig. 12. Impedances of the grid and MMC station of the stable case.

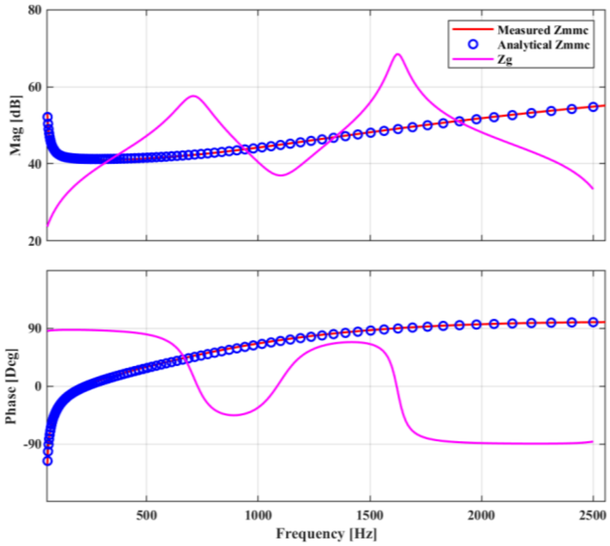

Fig. 13. Impedances of the grid MMC station of the unstable case.

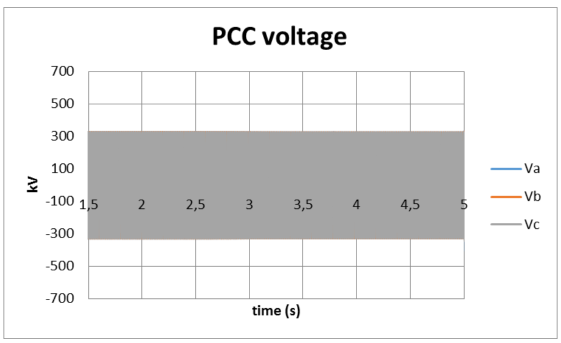

(a)

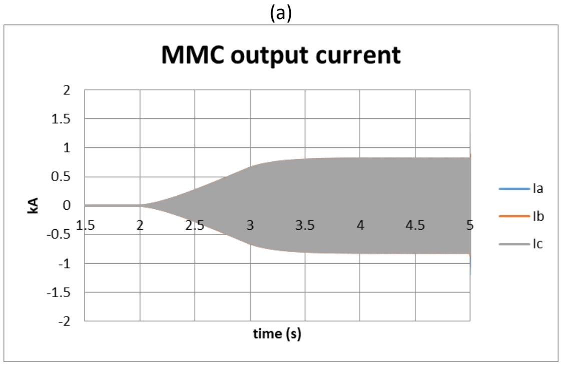

(b)

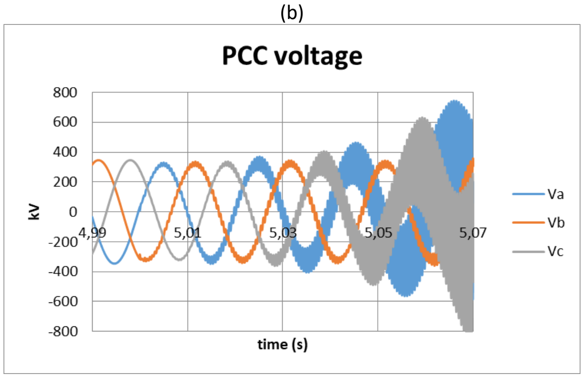

(c)

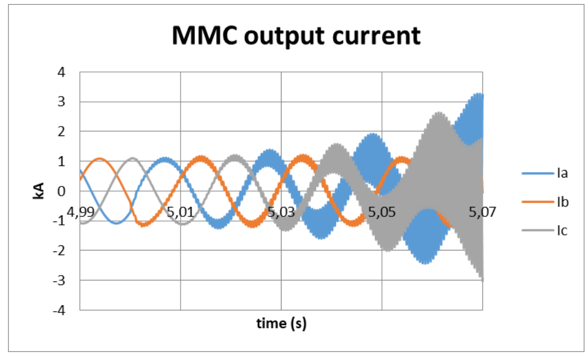

(d)

Fig. 14. Time domain simulation for energization of the MMC station and change in the grid configuration at 5 s which lead to unstable case.

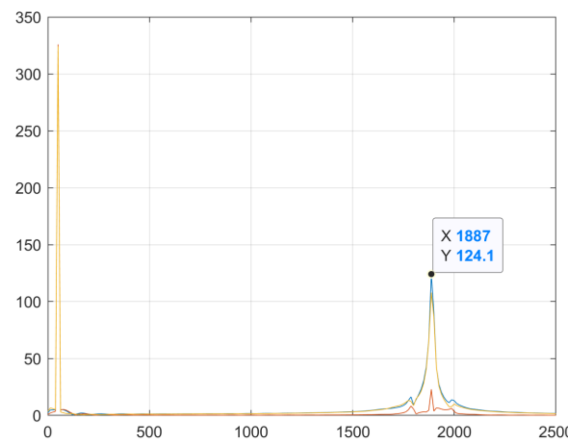

Fig. 15. FFT analysis of the unstable voltage waveforms.

References

[1] M. F. M. Arani and Y. A. R. I. Mohamed, "Analysis and performance enhancement of vector-controlled VSC in HVDC links connected to very weak grids," *IEEE Trans. Power Syst.*, vol. 32, no. 1, pp. 684–693, 2017.

[2] X. Wang and F. Blaabjerg, "Harmonic Stability in Power Electronic-Based Power Systems: Concept, Modeling, and Analysis," *IEEE Trans. Smart Grid*, vol. 10, no. 3, pp. 2858–2870, May 2019.

[3] C. Buchhagen, M. Greve, A. Menze, and J. Jung, "Harmonic stability-practical experience of a TSO," *Proc. 15th Wind Integr. Work.*, pp. 1–6, 2016.

[4] C. Zou et al., "Analysis of Resonance Between a VSC-HVDC Converter and the AC Grid," *IEEE Trans. Power Electron*., vol. 33, no. 12, pp. 10157–10168, Dec. 2018.

[5] Y. Wang, X. Wang, F. Blaabjerg, and Z. Chen, "Harmonic Instability Assessment Using State-Space Modeling and Participation Analysis in Inverter-Fed Power Systems," *IEEE Trans. Ind. Electron*., vol. 64, no. 1, pp. 806–816, Jan. 2017.

[6] L. Harnefors, M. Bongiorno, and S. Lundberg, "Input-Admittance Calculation and Shaping for Controlled Voltage-Source Converters," *IEEE Trans. Ind. Electron*., vol. 54, no. 6, pp. 3323–3334, Dec. 2007.

[7] D. Yang, X. Wang, and F. Blaabjerg, "Sideband Harmonic Instability of Paralleled Inverters With Asynchronous Carriers," *IEEE Trans. Power Electron*., vol. 33, no. 6, pp. 4571–4577, Jun. 2018.

[8] X. Yue, Z. Fang, F. Wang, Z. Zhang, and H. Shi, "A Novel Adaptive Frequency Injection Method for Power Electronic System Impedance Measurement," *IEEE Trans. Power Electron*., vol. 29, no. 12, pp. 6700–6711, Dec. 2014.